SAND2023-10861

SANDIA REPORT

Printed October 2023

Sandia National Laboratories

Pioneer WEC concept design report

Ryan G. Coe[1*], Jantzen Lee[1], Giorgio Bacelli[1], Steven J. Spencer[1], Kevin Dullea[1], Albert J. Plueddemann[2], Derek Buffitt[2], John Reine[2], Don Peters[2], Johannes Spinneken[3], Andrew Hamilton[4], Sahand Sabet[5], Salman Husain[5], Scott Jenne[5], Umesh Korde[6], Mike Muglia[7], Trip Taylor[7], Eric Wade[7]

[1]Sandia National Laboratories, *rcoe@sandia.gov
[2]Woods Hole Oceanographic Institution
[3]Evergreen Innovations
[4]Monterey Bay Aquarium Research Institute
[5]National Renewable Energy Laboratory
[6]Johns Hopkins University
[7]Coastal Studies Institute, East Carolina University

Prepared by
Sandia National Laboratories
Albuquerque, New Mexico 87185
Livermore, California 94550

Issued by Sandia National Laboratories, operated for the United States Department of Energy by National Technology & Engineering Solutions of Sandia, LLC.

Available to DOE and DOE contractors from

U.S. Department of Energy
Office of Scientific and Technical Information
P.O. Box 62
Oak Ridge, TN 37831

Telephone: (865) 576-8401
Facsimile: (865) 576-5728
E-Mail: reports@osti.gov
Online ordering: http://www.osti.gov/scitech

Available to the public from

U.S. Department of Commerce
National Technical Information Service
5301 Shawnee Road
Alexandria, VA 22312

Telephone: (800) 553-6847
Facsimile: (703) 605-6900
E-Mail: orders@ntis.gov
Online order: https://classic.ntis.gov/help/order-methods

ABSTRACT

The “Pioneer WEC” project is targeted at developing a wave energy generator for the Coastal Surface Mooring (CSM) system within the Ocean Observatories Initiative (OOI) Pioneer Array. The CSM utilizes solar photovoltaic and wind generation systems, along with rechargeable batteries, to power multiple sensors on the buoy and along the mooring line. This approach provides continuous power for essential controller functions and a subset of instruments, and meets the full power demand roughly 70% of the time. Sandia has been tasked with designing a wave energy system to provide additional electrical power and bring the CSM up-time for satisfying the full-power demand to 100%. This project is a collaboration between Sandia and Woods Hole Oceanographic Institution (WHOI), along with Evergreen Innovations, Monterey Bay Aquarium Research Institute (MBARI), Eastern Carolina University (ECU), Johns Hopkins University (JHU), and the National Renewable Energy Laboratory (NREL). This report captures Phase I of an expected two phase project and presents project scoping and concept design results.

CONTENTS

Executive summary 11

1. Introduction 13
   1.1. Pioneer Array Coastal Surface Mooring system 13
   1.2. Design requirements 16

2. Background 19
   2.1. Site conditions 19
   2.2. Base system analysis 21
      2.2.1. Power generation and loads 21
      2.2.2. Hydrodynamics 23

3. WEC concepts 27
   3.1. Concept A1: sliding mass 27
   3.2. Concept A2: pitch resonator 28
   3.3. Concept B1: in-line PTO 31

4. Conclusions and future work 35

References 39

A. Battery state of charge estimation 41

B. Deployment sequence 45

C. Other wave energy concepts 47

Distribution 48

LIST OF FIGURES

Figure 1-1. Coastal Pioneer Array sensor platforms. 14
Figure 1-2. Pioneer Array Central Surface Mooring layout details. 15
Figure 1-3. Pioneer Array Central Surface Mooring system components. 15
Figure 2-1. Pioneer Array Coastal Surface Mooring proposed mid-Atlantic Bight deployment location shown along with historical measurement locations. 19
Figure 2-2. Mid-Atlantic Bight deployment location wave conditions. 20
Figure 2-3. Correlations of in-situ observation data at PEACH B1. 21
Figure 2-4. Central Surface Mooring system power generation and state of charge monthly performance at New England Shelf deployment. 22
Figure 2-5. Central Surface Mooring system power generation and state of charge weekly performance at New England Shelf deployment. 23
Figure 2-6. Central Surface Mooring buoy response spectra from New England Shelf deployment. 24
Figure 2-7. Central Surface Mooring buoy New England Shelf deployment response spectra as a function of sea state peak period. 24
Figure 2-8. Central Surface Mooring buoy pitch motion from New England Shelf deployment. 25
Figure 3-1. Wave energy converter design concept categories considered. 27
Figure 3-2. Sliding mass wave energy converter concept. 28
Figure 3-3. Pitch resonator wave energy converter concept. 29
Figure 3-4. In-line power take-off wave energy converter concept. 31
Figure 3-5. Stretch hose strain behavior with local linear approximations. 32
Figure 3-6. In-line PTO concept mechanical power generation based on motion and tension fluctuation amplitude. 34
Figure A-1. Peukert curve for 4-P GPL-4DL absorbent glass mat battery. 41
Figure A-2. Battery voltage versus depth of charge. 42
Figure B-1. Coastal Surface Mooring deployment sequence. 45
Figure B-2. Coastal Surface Mooring deployment sequence (cont.). 46
Figure C-1. Other wave energy converter concepts considered. 47

LIST OF TABLES

Table 1-1. Pioneer WEC project phases. 13
Table 1-2. Pioneer Array Central Surface Mooring system key parameters. 16
Table 2-1. Central Surface Mooring system power generation statistics at New England Shelf deployment. 23
Table 3-1. Linear rack and pinon moving mass concept analysis results. 28
Table 3-2. Proteus-DS modeling results for Coastal Surface Mooring in 100 m water at Mid-Atlantic Bight. 33
Table 4-1. Wave energy converter system concept assessment matrix. 36
Table A-1. Battery state of charge analysis of variance. 43

EXECUTIVE SUMMARY

This project is targeted at delivering and integrating a wave energy generation system into the Coastal Surface Mooring in order provide additional electric power. Drawing on the project scoping and concept design analyses, a summary of leading wave energy design concepts is presented in Table 4-1. Based on these findings, our team currently views Concept A2 (“pitch resonator”) as the most promising concept, followed by Concept B1 (“in-line power take-off”). The next steps for this project should be to down-select to a single design concept and then pursue the detailed design, assemble a prototype, perform shakedown and integration testing, and deploy a wave energy equipped Coastal Surface Mooring system for at-sea testing.

1. INTRODUCTION

This report captures the current status and work to-date on a project to design, build, and deploy a wave energy converter (WEC) for the Pioneer Array[1] Coastal Surface Mooring (CSM) system within the National Science Foundation (NSF) sponsored Ocean Observatories Initiative (OOI)[2]. The high-level goals of this project are:

1. Provide an additional power source for the CSM system to augment the existing solar and wind generators, thus increasing the ability of the system to meet the current full-power demand and potentially expanding the ability to host sensors with higher power demands
2. Create publicly available documents and data on the design, testing, and performance of the WEC system developed for the CSM system in order to support ongoing and future development of WECs for blue economy power at-sea applications

This report covers the work completed for Phase I of an anticipated two phase project (see Table 1-1). Phase I is focused on project scoping, defining design requirements, and the development of concept designs. Phase II will down-select to 1-2 concept designs and pursue detailed design, assembly, testing and ocean deployment of these systems.

1.1. Pioneer Array Coastal Surface Mooring system

The Pioneer Array is one of three moored arrays operated by Coastal and Global Scale Nodes (CGSN) team from Woods Hole Oceanographic Institution (WHOI) for the OOI program.

- Coastal Pioneer Array:[1] Originally deployed near deployed on the New England shelf about 70 nm south of Martha's Vineyard (referred to herein as the "New England Shelf" deployment), the Coastal Pioneer array is proposed to be redeployed at the Southern Mid-Atlantic Bight (MAB) between Cape Hatteras and Norfolk Canyon in 2024.
- Global Irminger Array:[3] The Global Irminger Sea Array in the North Atlantic is located in a region with strong wind and large waves driving atmosphere-ocean exchange and is characterized by high biological productivity. It is one of the few places on Earth with deep-water formation that feeds the large-scale thermohaline circulation.

[1] https://oceanobservatories.org/array/coastal-pioneer-array/
[2] https://oceanobservatories.org/
[3] https://oceanobservatories.org/array/global-irminger-sea-array/

Table 1-1 Pioneer WEC project phases.

Phase	Time period	Description
Phase I	January - July 2023	Project scoping and concept design
Phase II	August 2023 - 2027	Detailed design, assembly, testing, deployment, and final reporting

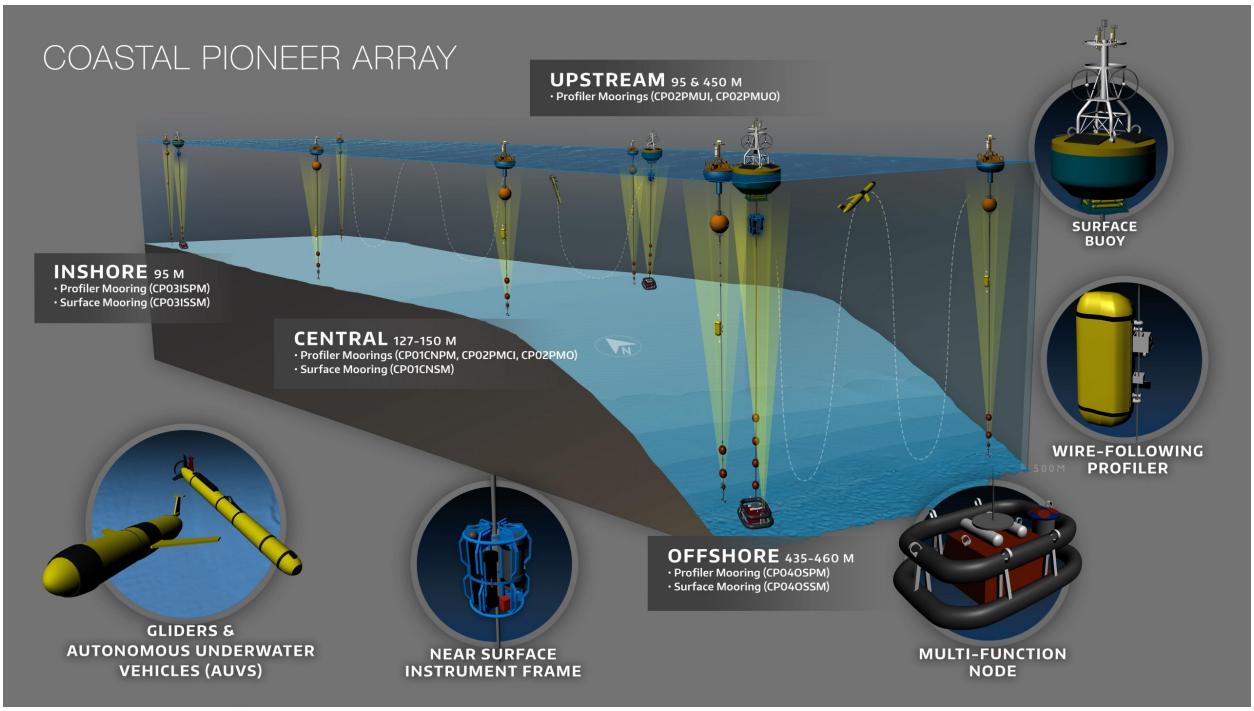

Figure 1-1 Coastal Pioneer Array sensor platforms (reproduced from `https://oceanobservatories.org/array/coastal-pioneer-array/`).

- Global Papa Array:[4] The Global Station Papa Array is located in the Gulf of Alaska in an area vulnerable to ocean acidification, and is characterized by a productive fishery and low eddy kinetic energy.

The Pioneer Array includes a mixture of different sensing platforms (see Figure 1-1). Within the Pioneer Array, our project is focused on the CSM system (see Figure 1-3). The CSM system is specifically designed to take measurements in the continental shelf and slope, where a dynamic exchange of nutrients, pollutants, and biomatter between the coast and deep ocean takes place. The system comprises a surface buoy (Figure 1-3a), "Near-Surface Instrument Frame (NSIF)" located about 7 m below free surface (Figure 1-3b), and seafloor "Mutli-Function Node (MFN)" (Figure 1-3c). The mooring system uses multiple sections of electromechanical (EM) stretch hose [21, 22, 15, 11], which enables the buoy to move freely in waves.

[4] https://oceanobservatories.org/array/global-station-papa-array/

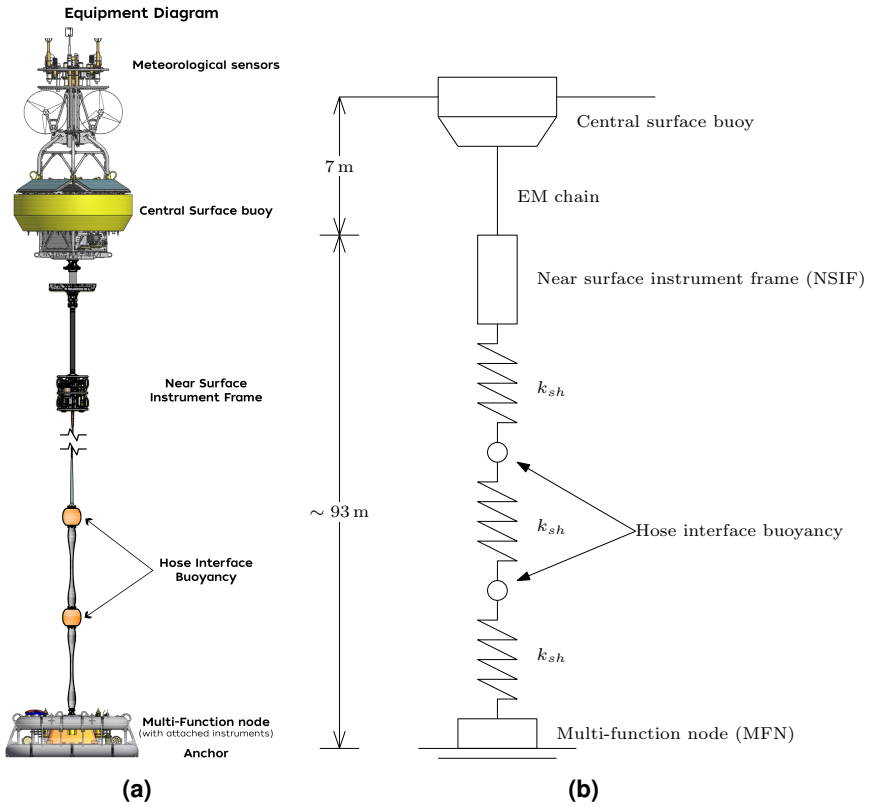

Figure 1-2 Pioneer Array Central Surface Mooring layout details.

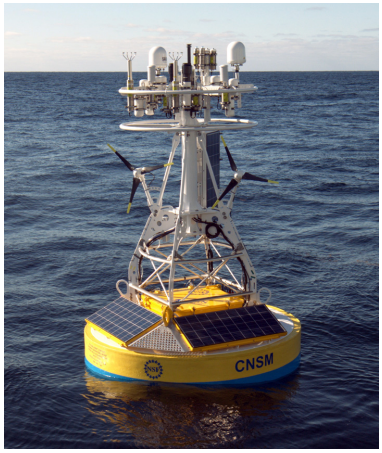

(a) Surface buoy

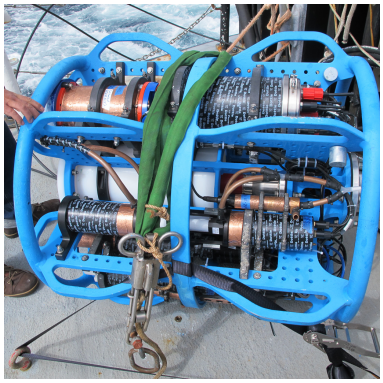

(b) Near surface instrument frame (NSIF)

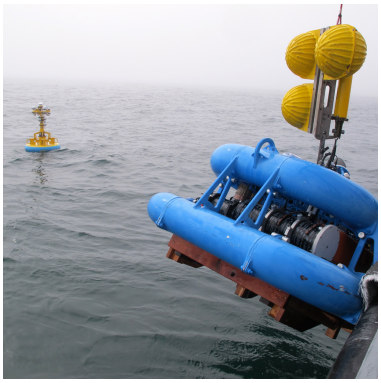

(c) Multi-function node (MFN)

Figure 1-3 Pioneer Array Central Surface Mooring system components.

Table 1-2 Pioneer Array Central Surface Mooring system key parameters.

Parameter	Value	Notes
Nominal deployment location	35.943117, -74.88035	
Water depth	89 m	
Median wave energy period	5.3 s	Data: WPTO Hindcast
Median sig. wave height	1.6 m	Data: WPTO Hindcast
Median spectral width (IEC)	0.32	Data: WPTO Hindcast, $\nu = \sqrt{\frac{m_0 m_2}{m_1^2} - 1}$
Buoy diameter	3.3 m	
Buoy mass	3747 kg	
NSIF mass	207.8 kg	
Anchor mass	3000 kg	Deadweight
Power consumption	50-100 W	
Batteries	Twelve (12) GPL-4DL Lifeline AGM batteries	24 V bus voltage; 840 AH capacity; 20 Hr rate
Wind turbines	Two (2) Superwind SW350 350W wind turbines	Some modifications made; SCR24 PWM diversion charge controller and 350 W dump resistor
Solar panels	Four (4) 140 W 12 V Kyocera KD-140 PV panels	Genasun GVB-8-Pb-24CV PV boost charge controllers
Maintenance cycle period	recovered/deployed every 6 months	AUV survey every 2 months

Key system specifications are listed in Table 1-2. The surface buoy hosts two (2) wind turbines and four (4) solar panels (see Figure 1-3a) along with a rechargeable battery system. Connections from the surface buoy provide power and communications to the NSIF, and MFN. These power sources support an average load of 50-100 W (see Section 2.2.1 for a more detailed discussion of power generation and loads). The existing wind turbines and solar panels meet the full power demand of the CSM roughly 70% of the time. True blackouts due to insufficient power levels are exceedingly rare. Instead, the system is manually throttled (i.e., lower priority power demands are shut off) to maintain overall system operation during periods where battery/generation power levels cannot meet demand. Nonetheless, these "brownouts" are undesirable and may potentially be alleviated via a wave energy system.

1.2. Design requirements

Design requirements and constraints have been developed via discussions between WHOI and the remainder of the Pioneer WEC team. These requirements were informed by qualitative experiences and quantitative analysis of data from the previous New England Shelf deployment of the Pioneer Array. While the design requirements and constraints are generally flexible and interdependent, there are five key requirements guiding this project:

1. **Generate power:** Electrical power generation levels on the order of 10-100 W would be relevant and beneficial to the functionality of the CSM system. Power generated during periods of low wind and solar power would be more beneficial. Also, since existing generation assets and the battery storage system are located at the surface buoy, and since losses to transmit power down ~ 100 m to the MFN are nontrivial, power generation proximate to power use would be desirable. This could include generation on the buoy (to service buoy and NSIF sensors) and/or on the MFN.
2. **Avoid catastrophic failures:** Any failures in the WEC shall not create cascading failures in the remainder of the system, which could lead to structural failure of the mooring and thus compromise the the scientific measurement mission of the system.
3. **Safe mode:** The wave energy device shall have "safe mode" which can be activated for deployment, recovery, and during storm events to prevent damage to equipment and minimize hazards to personnel during operations.
4. **Not affect measurements:** Scientific measurement is the central mission of the system. The WEC therefore shall minimize adverse effects to these measurements (e.g., by causing excessive motion, interfering with current flow, blocking the measurement path of a sensor, blocking the free flow of water through a port or pump, creating heat, or otherwise changing water ambient water properties). Note that sea state estimation is a key measurement, so even *reductions* in CSM motion may need to be considered in order to determine if their effect beneficial or even acceptable.
5. **Minimize changes to operational requirements:** To the degree possible, changes which increase deployment, operational, or maintenance beyond current requirements (i.e., ship size, deployment/recovery time, etc.) should be minimized/avoided.

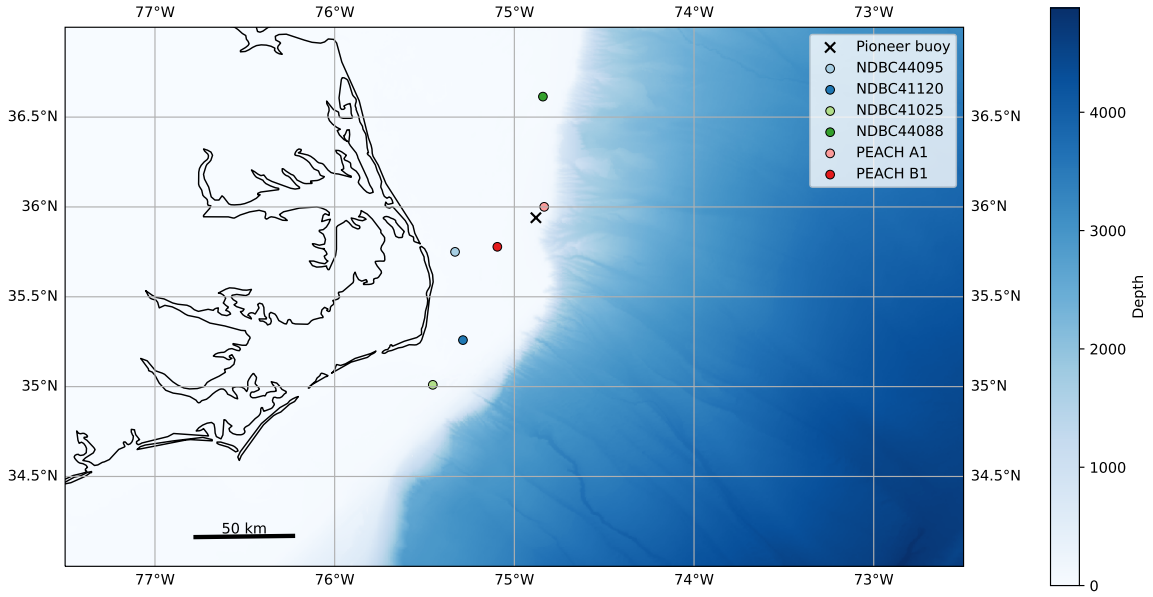

Figure 2-1 Pioneer Array Coastal Surface Mooring proposed mid-Atlantic Bight deployment location shown along with historical measurement locations.

2. BACKGROUND

2.1. Site conditions

To scope the relocation of the Pioneer Array to the MAB, WHOI performed a detailed site characterization [23]. The proposed MAB deployment site for CSM system targeted in this project is shown in Figure 2-1 along with nearby historical measurement locations. An initial site conditions characterization was performed using hindcast data [1]. Figure 2-2a shows a joint probability distribution for the significant wave height and energy period. Significant wave height and wind speed vary throughout the year with summer months being the least active. Reduced activity in the summer is due to the lower occurrence of major storms such as nor'easters or hurricanes. The most common sea state has a significant wave height of 1.6 m and an energy period 5.3 s. Referring to the mean monthly conditions in Figure 2-2c, we can see that the energy period is relatively consistent throughout the year, whereas the significant wave height varies by as much as 100%.

Extreme waves due to hurricanes are a concern in the proposed MAB deployment location. From Figure 2-2b, we can see that sea states with a significant wave height on the order of 7 m are expected for only a 1-year return period. Considering the individual wave heights close to twice the significant wave height can easily occur, the design should consider individual waves as high as 14 m. These predictions are generally in line with the analysis performed to scope the relocation of the Pioneer Array to the MAB and ensure survival of different moorings and assets with the Array [23].

Using the coincident measurements taken by the PEACH B1 buoy, a correlation analysis was performed (see Figure 2-3). Aside from some intuitive correlations between solar irradiance and

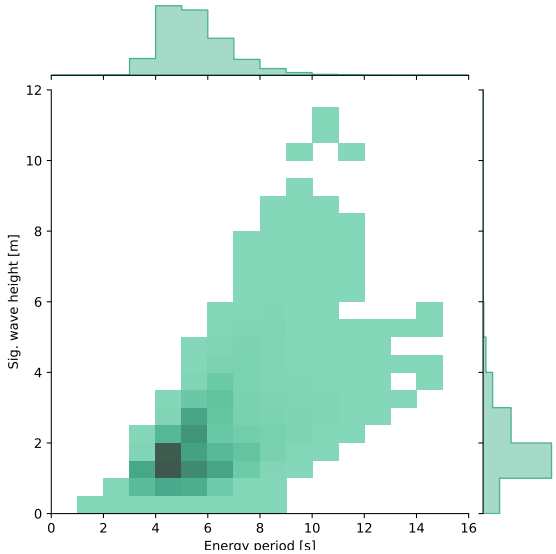

(a) Sea state joint probability distribution.

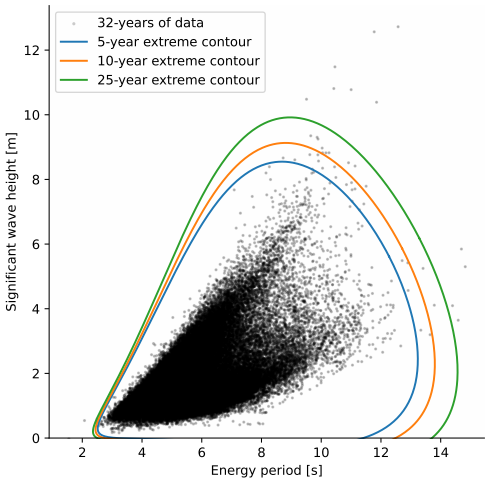

(b) Extreme sea state contours.

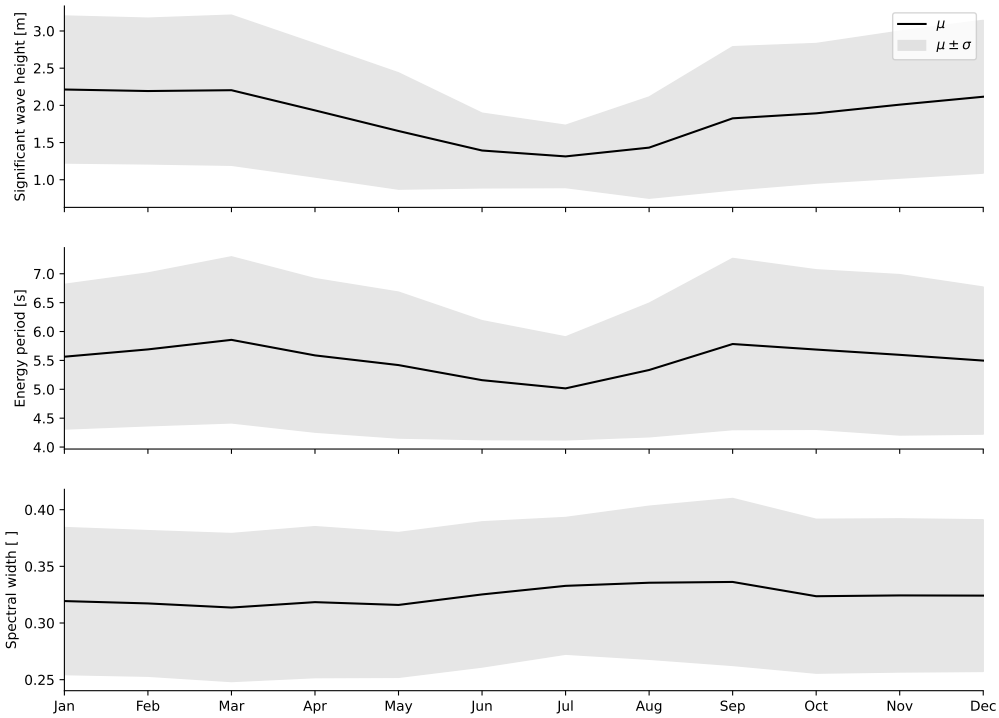

(c) Mean monthly waves conditions with 1 standard deviation error bars.

Figure 2-2 Mid-Atlantic Bight deployment location wave conditions.

Correlation (R)	waveHs (m)	waveTp (s)	Wind Speed (m/s)	pir (w/m^2)	psp (w/m^2)	Surface Flow Speed (m/s)	Surface East Velocity (m/s)	Surface North Velocity (m/s)	Air Temp (C)	Surface Water Temp (C)	Bottom Water Temp (C)	Water Level (m)
Significant Wave Height (m)	1	0.277	0.659	-0.072	-0.188	0.338	0.102	-0.244	-0.204	-0.244	-0.203	-0.244
Peak Period (s)	0.277	1	-0.101	-0.082	-0.036	0.038	-0.041	-0.233	-0.029	-0.112	0.179	0.022
Wind Speed (m/s)	0.659	-0.101	1	-0.124	-0.125	0.356	0.1	-0.158	-0.249	-0.164	0.086	0.025
pir (w/m^2)	-0.072	-0.082	-0.124	1	0.089	-0.033	0.113	0.111	0.778	0.695	0.044	0.03
psp (w/m^2)	-0.188	-0.036	-0.125	0.089	1	-0.027	-0.1	-0.036	0.189	0.107	-0.107	-0.027
Surface Flow Speed (m/s)	0.338	0.038	0.356	-0.033	-0.027	1	0.096	-0.352	-0.064	-0.077	0.032	-0.044
Surface East Velocity (m/s)	0.102	-0.041	0.1	0.113	-0.1	0.096	1	-0.041	0.109	0.006	-0.138	-0.013
Surface North Velocity (m/s)	-0.244	-0.234	-0.158	0.111	-0.036	-0.352	-0.041	1	0.214	0.135	-0.101	0.201
Air Temperature (C)	-0.204	-0.029	-0.249	0.778	0.189	-0.064	0.109	0.214	1	0.791	-0.113	-0.055
Surface Water Temp (C)	-0.244	-0.112	-0.164	0.695	0.107	-0.077	0.006	0.135	0.791	1	0.308	0.088
Bottom Water Temp (C)	-0.203	0.179	0.086	0.044	-0.107	0.032	-0.138	-0.101	-0.113	0.308	1	0.023
Water Level (m)	-0.244	0.022	0.025	0.03	-0.027	-0.044	-0.013	0.201	-0.055	0.088	0.023	1

Figure 2-3 Correlations of in-situ observation data at PEACH B1.

air/water temperatures, we see a notable correlation (0.659) between the significant wave height and wind, indicating that a large proportion of waves in this area area due to local storms. This finding generally limits the degree to which a wave energy system might be designed to operate optimally in conditions when winds are at a lull, as wind and wave energy at the proposed MAB deployment site generally coincide.

2.2. Base system analysis

A series of analyses of the "base system" (i.e., the CSM with no wave energy system added) were performed to inform the wave energy design process. Section 2.2.1 presents an accounting of power generation and the battery state of charge during the New England Shelf deployment. Section 2.2.2 presents analyses of the CSM dynamics and hydrodynamics based on measurements taken during the New England Shelf deployment.

2.2.1. Power generation and loads

The past performance of the CSM power system can be analyzed using historical data from the New England Shelf deployment[5]. Figure 2-4 shows the monthly average performance with ± 1 standard deviation of the wind and solar PV generation systems along with the estimated battery state of charge (SoC), which was estimated by

$$V_{oc} = V + 0.368I \tag{1a}$$

$$\text{SoC} = \frac{100}{2.4}(V_{oc} - 23.16). \tag{1b}$$

[5]Data from deployments 5-9, which span from May 2016 to April 2022 were used in this analysis

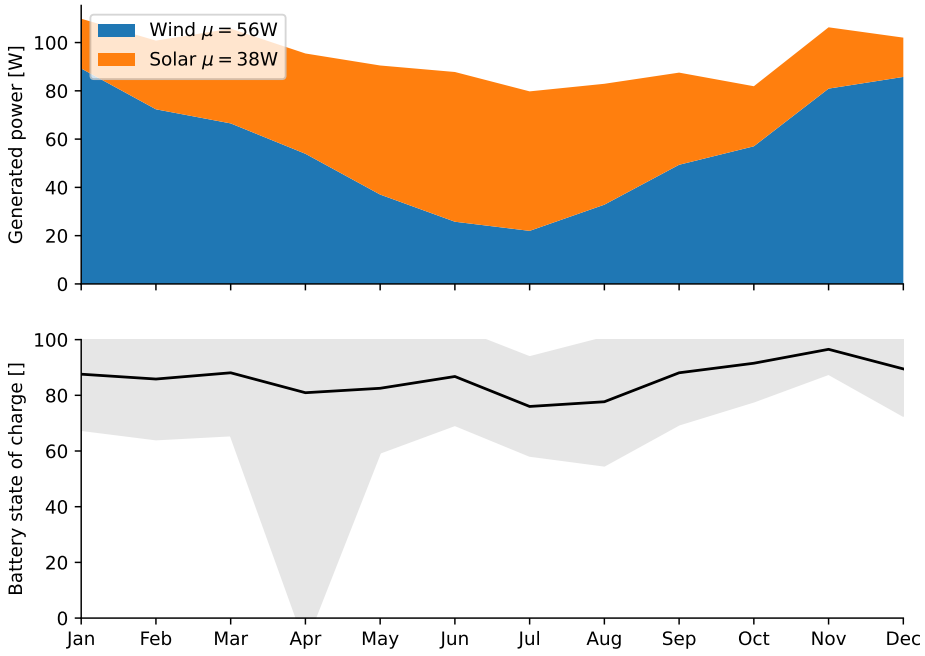

Figure 2-4 Central Surface Mooring system power generation and state of charge monthly performance at New England Shelf deployment (2016-2022).

Here, V and V_{oc} are the voltage and open circuit voltage and I is the current. A detailed explanation of (1) is provided in Appendix A.

From Figure 2-4, we can see that wind and solar PV provide complimentary generation performance, with the wind generation being at its peak in winter months and the solar generation peaking in summer months. This results in a relatively stable 100 W mean generation ($\sigma = 10$ W) from month to month, which is generally sufficient to keep the battery state of charge close to 100%. However, the contribution from wind is roughly 50% greater than that from solar generation, and thus the greatest generation vs. demand deficit occurs when the winds are reduced in the summer months. From Figure 2-4, we can see that, in terms the average performance, an additional ~ 20 W of power would likely achieve an SoC close to 100%.

In Table 2-1, we see that individually both the wind and solar generation vary dramatically from one day to the next, with coefficients of variation ($CV = \mu/\sigma$) close to unity. Fortunately, the relative variation in total generation is substantially lower ($CV = 0.5$), indicating again that the wind and solar resources tend to be somewhat complementary in nature (the Pearson correlation coefficient on the daily mean generation between wind and solar is only 0.17).

Figure 2-5 gives a weekly accounting of the power system performance during the New England Shelf deployment. The upper set of axes show the *mean* weekly power generation from the wind and solar PV systems while the lower set of axes show the *minimum* SoC for each week. Note that, as discussed in Section 1.1, the CSM power loads are sometimes throttled when generation/battery

Table 2-1 Central Surface Mooring system power generation statistics at New England Shelf deployment (2016-2022).

	Mean (daily)	STD (daily)	Max. monthly avg.	Min. monthly avg.
Wind	58 W	54 W	112 W (Dec., 2017)	18 W (July, 2020)
Solar	37 W	26 W	73 W (July, 2019)	11 W (Dec., 2016)
Total	95 W	48 W	128 W (Jan., 2022)	66 W (Oct., 2021)

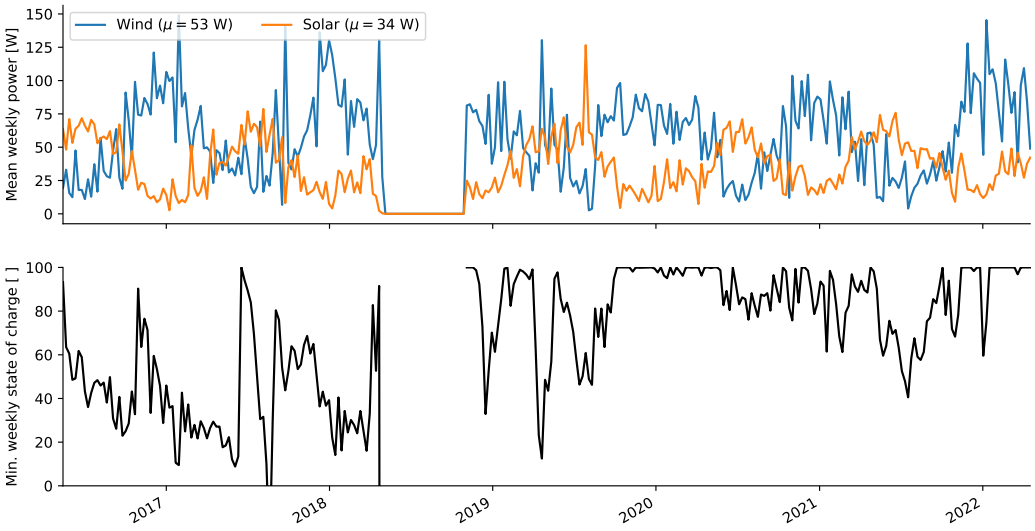

Figure 2-5 Central Surface Mooring system power generation and state of charge weekly performance at New England Shelf deployment (2016-2022; note there is a gap in data from 2018.)

energy levels cannot meet demand – this throttling likely occurs multiple times in the time series shown in Figure 2-5. From Figure 2-5, we can see the low battery SoC appears to be mostly correlated with lower wind generation.

Relative to the New England Shelf deployment location, the metocean conditions at the MAB proposed deployment site are very similar. As part of the planning the proposed MAB deployment, a site characterization was performed [23] that indicated the mean currents, wave heights, and wind are comparable to the the original New England Shelf site.

2.2.2. Hydrodynamics

The CSM buoy has a 3DM-GX3-25 Attitude Heading Reference System (AHRS) that can be used to estimate the buoy's motion. Figure 2-6a shows the heave, pitch, and roll accelerations of the CSM buoy during the New England Shelf deployment. From Figure 2-6a, we can see that the heave response is relatively broad-banded, with a flat response for waves with periods greater than

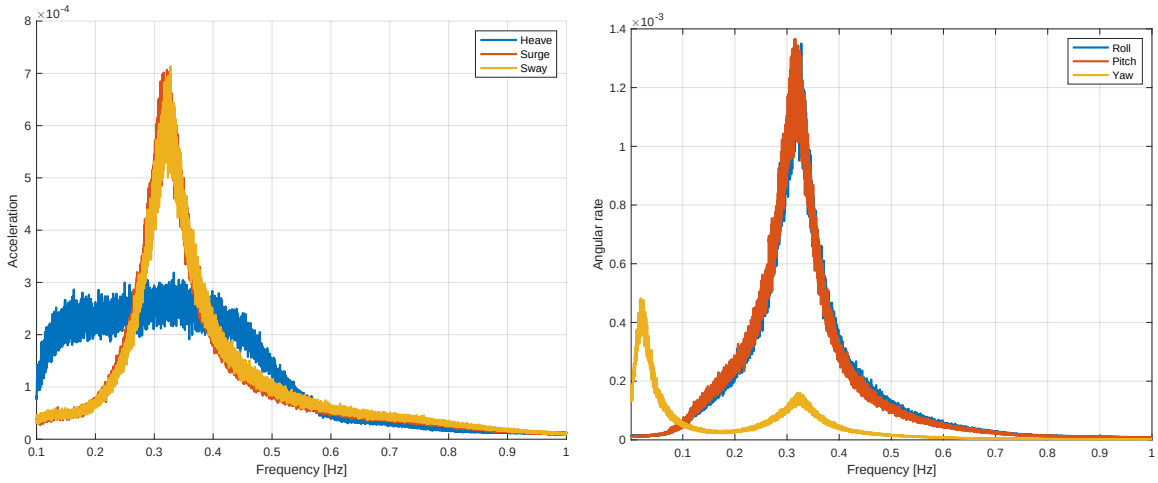

(a) Linear motion **(b) Angular motion**

Figure 2-6 Central Surface Mooring buoy response spectra from New England Shelf deployment.

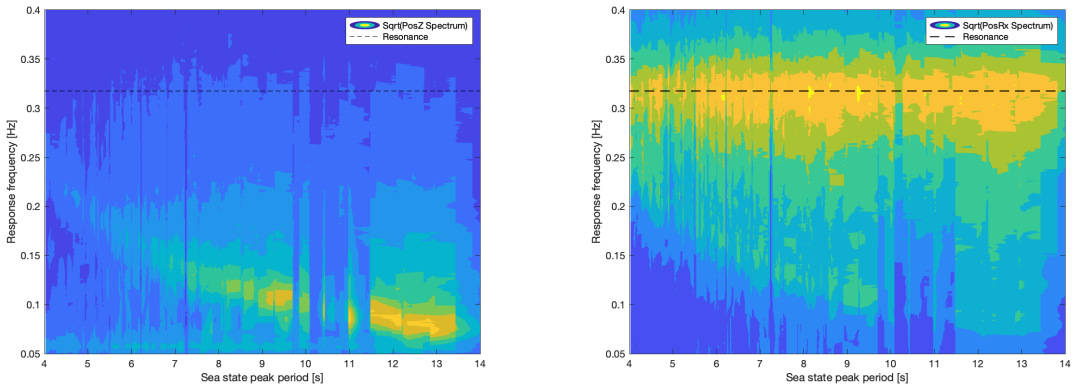

(a) Linear motion **(b) Angular motion**

Figure 2-7 Central Surface Mooring buoy New England Shelf deployment response spectra as a function of sea state peak period.

2 s (< 0.5 Hz). The pitch and roll responses (see Figure 2-6b) are nearly identical, as expected, and show very sharp lightly damped resonances at approximately 3.1 s (0.32 Hz).

The sensitivity of these different responses to varying sea state conditions is illustrated in Figure 2-7. The pitch/roll response is shown in Figure 2-7b. While there is some broadening of the response that occurs as the peak period of the incident sea state increase, the pitch/roll response is relatively insensitive to the incident sea state, with the response remaining relatively narrow-banded with a peak at the resonance of ~ 0.32 Hz. Conversely, we can see that the heave response is quite sensitive to the sea state, with the peak response closely following the sea state's peak, as would be expected for a small heaving body.

The data in Figure 2-7b can also be analyzed to assess the statistical response in a traditional two dimensional grid based on significant wave height and peak period (see Figure 2-8). From Figure 2-8, we can see that pitch motion of the buoy has almost no sensitivity to the sea state's

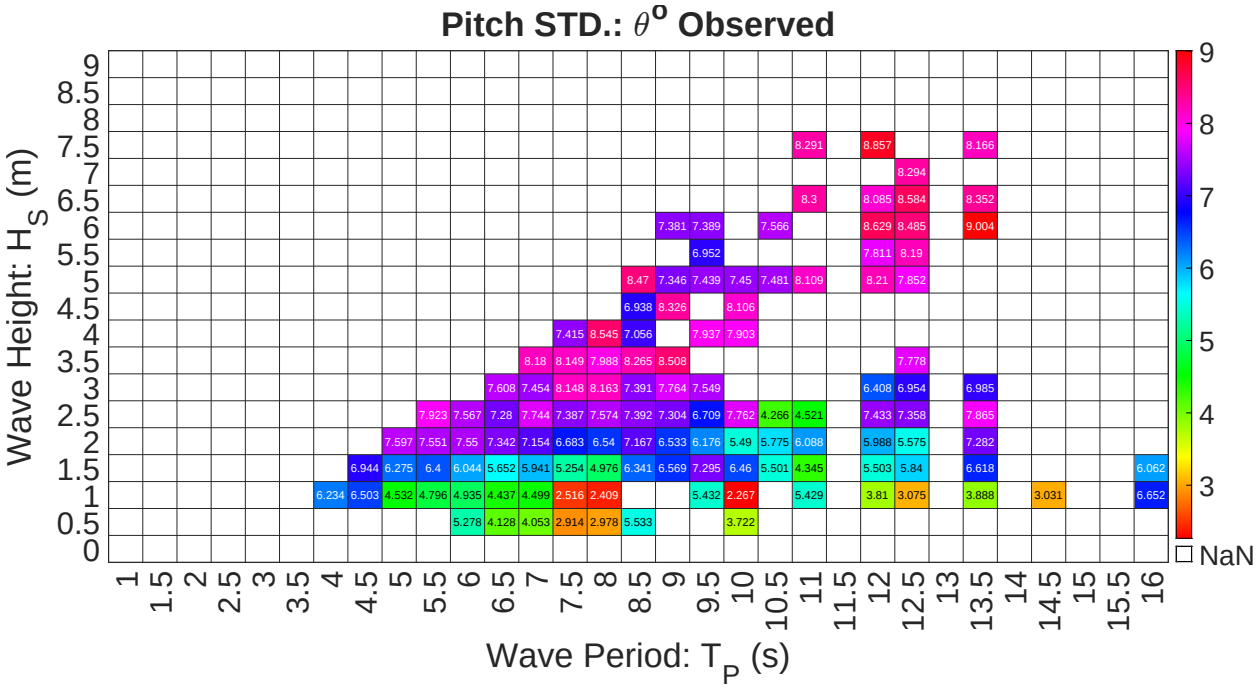

Figure 2-8 Central Surface Mooring buoy pitch motion from New England Shelf deployment.

peak period and is also relatively insensitive to the significant wave height. A 3 s deep water wave is approximately 14 m long, meaning that for a wave breaking steepness limit of 1/7, waves of this period are unlikely to exceed a height of 2 m, even in the largest storms. This creates a potentially important saturation effect for a body that responds to these short period waves (i.e., even in the largest storms, the amplitude of 3 s waves is limited to 2 m, meaning that the pitch excitation at its natural frequency is also limited).

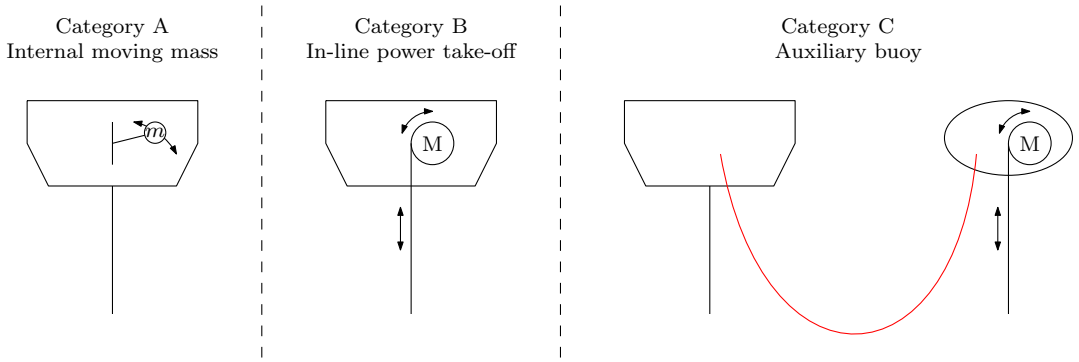

Figure 3-1 Wave energy converter design concept categories considered.

3. WEC CONCEPTS

Figure 3-1 shows three categories of WEC design concepts considered. After initial discussion, Concept C was removed from consideration due to the additional deployment and operational challenges (e.g., seafloor cable laying and underwater connectors) that such a system would require. Additional concepts were also discussed, but discarded for various reasons – see Appendix C. Thus, two main concept categories shown as A and B in Figure 3-1 will be considered within this project.

Category A encompasses "internal moving mass" systems and Category B captures "in-line power take-off" systems. Systems falling within Category B (see, e.g., [9, 12]) have generally received much more attention from both researchers and private developers than Category A concepts [8, 14]). At a high level, Category A concepts are expected to deliver lower power levels [16], but the concepts should be easier to integrate into the mature CSM design than Category B concepts. In the following sections, we explore three design concepts from Category A and Category B in further detail.

3.1. Concept A1: sliding mass

Within Category A, a linear sliding mass concept, as shown in Figure 3-2, was considered. In this concept, a mass would be mounted on a linear track with a positive stiffness spring and a motor/generator that acts as a damper. The pitch/roll motion of the buoy would cause the mass to translate back and forth along the linear track, allowing the motor/generator to extract power.

If the moving mass is small relative to the mass of the buoy, it can be assumed that the motion of the mass will have a negligible effect on buoy motion. A high level assessment along these lines was performed using the linear rack and pinon system proposed by [4]. To bracket the potential performance, motion data from January and June of the Pioneer Array's New England Shelf deployment were used. From the results shown in Table 3-1, we can see that the mechanical power ranges from 41 to 95 W. An optimistic estimate for the mechanical to electrical power conversion efficiency of 25-50% brings this estimate just within the range of viability according the design requirements defined in Section 1.2. The mechanical power levels predicted by the two-body model

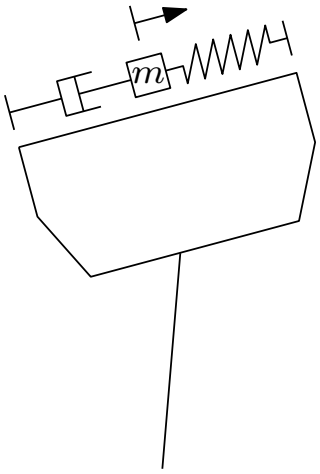

Figure 3-2 Sliding mass wave energy converter concept.

Table 3-1 Linear rack and pinon moving mass concept analysis results.

Parameter	January	June
Sig. wave height [m]	2.37	1.03 (43% of Jan)
Inc. wave power [kW/m]	30.25	4.11 (14% of Jan)
Standard dev. of buoy angle [deg]	6.7	4.3 (64% of Jan)
Mechanical power [W]	95	41 (43% of Jan)

were similar to the simplified model (10-100 W depending on stroke length, friction, etc.). A more detailed model, in which the coupled dynamics for the two-body system (i.e., body 1 is the buoy and body 2 is the moving mass), was also developed.

A linear sliding mass wave energy system would have the advantage of acting as a low-pass filter, responding relatively consistently to frequencies below some resonance. However, this advantage may be somewhat diminished by the fact that the CSM buoy tends to respond consistently with a very narrow response (see Section 2.2.2). The location of the linear track would impact the performance of the wave energy system and would also affect the response dynamics of the CSM buoy. To maximize the generated power, the length of the linear track would on the order of 2.5 m and have minimal friction. Coupling effects due to heave, surge, sway, and yaw of the buoy have not yet been analyzed, but would generally increase the complexity of system dynamics.

3.2. Concept A2: pitch resonator

Figure 3-3 shows a second Category A moving mass wave energy system concept, referred to herein as a pitch resonator, where a flywheel (J_{pto}) coupled to the buoy via a positive stiffness spring (k_{pto}) rotates due to the pitching motion of the buoy. A motor/generator is employed in parallel with the spring to harvest power from the system. The motor/generator would be generally capable of operating in four quadrants (i.e., acting as either a motor or generator), however, it would

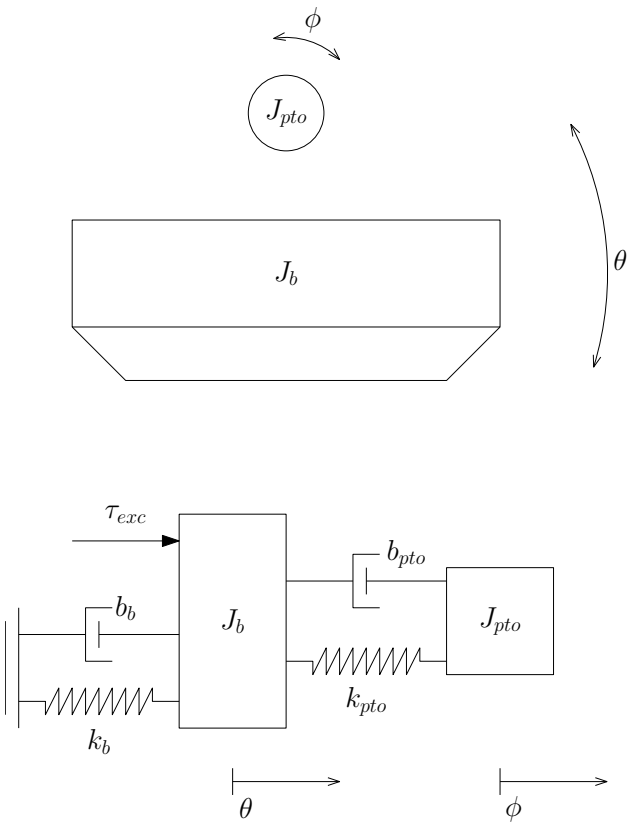

Figure 3-3 Pitch resonator wave energy converter concept (upper: physical appearance; lower: dynamic system shown as linear motion system for better clarity).

typically operate as a pure damper (see b_{pto} in Figure 3-3). Figure 3-3 contains two illustrations of the concept: the top portion of the figure shows the physical appearance while the bottom portion of the figure shows the dynamic system (note that while the motion of the system is rotation, this lower portion of Figure 3-3 uses linear interpretation for better clarity).

This concept is somewhat similar to pendulum concepts that have been pursued for WECs (see, e.g., [5, 18, 20, 10, 7]), but is notably unique in that the flywheel has its center of gravity at the center of rotation. With center of gravity collocated with the center of rotation, only moments (not forces) result in relative motion between the buoy and flywheel. In addition to avoiding the coupling of heave/surge to pitch/roll, this design decision also eliminates the chaotic behavior associated with a double pendulum system [24, 7] and the challenges therein. While it is physically a rotational system, the pitch resonator can be conceptually thought of as the angular equivalent to a classic tuned mass damper (see lower portion of Figure 3-3) [6, 19]. The governing equations of motion describing the system would be

$$(J_b + J(\omega))\ddot{\theta} = \tau_{exc} - k_b\theta - b_b(\omega)\dot{\theta} - k_{pto}(\theta - \phi) - b_{pto}(\dot{\theta} - \dot{\phi}) \tag{2a}$$

$$J_{pto}\ddot{\phi} = k_{pto}(\theta - \phi) + b_{pto}(\dot{\theta} - \dot{\phi}), \tag{2b}$$

where the resonant frequency of the PTO system would be

$$\omega_n = \sqrt{k_{pto}/J_{pto}}. \tag{3}$$

In the event that volumetric or mass-based design constraints infringe on the proper tuning of spring to mass ratio, a transmission ratio can be incorporated between the spring and the flywheel, with the transmission being grounded to the buoy. In this way, the equations of motions would be modified to incorporate the transmission ratio accordingly.

$$(J_b + J(\omega))\ddot{\theta} = \tau_{exc} - k_b\theta - b_b(\omega)\dot{\theta} - N^2 k_{pto}(\theta - \phi) - b_{pto}(\dot{\theta} - \dot{\phi}) \tag{4a}$$

$$J_{pto}\ddot{\phi} = N^2 k_{pto}(\theta - \phi) + b_{pto}(\dot{\theta} - \dot{\phi}) \tag{4b}$$

The resulting resonant frequency would be

$$\omega_n = N\sqrt{k_{pto}/J_{pto}}. \tag{5}$$

In any configuration, such a concept would be narrow-banded in its frequency response, as it is inherently acting as a resonator. However, due to the narrow-banded pitching/rolling response of the buoy itself (see Section 2.2.2), a properly tuned resonance would allow for efficient and non-negligible power generation from the pitching of the buoy.

The physical implementation of the pitch resonator concept could be designed as an entirely self-contained bolt-on system, with the only opportunity for ingress of water and debris being static face sealing gaskets and power cables entering and leaving the system. No dynamic seals would be required, significantly cutting down on losses due to friction. Such a system could be designed using a continuous travel magnetic spring [3], which would eliminate the presence of positional limits and potentially reduce fatigue issues. A design without travel limits would have at least two key benefits:

1. Firstly, during heavy pitching of the buoy (i.e., during a storm), the WEC will not need to throttle its motion to mitigate over-travel issues. In fact, because of its quasi-infinite travel, during such conditions, the WEC could stay active and help to mitigate damage to the buoy and its sensors by taking kinetic energy out of the system.

2. Secondly, having the infinite travel magnetic spring at the center of the design would eliminate the presence of positional hard-stops. This would decrease (if not eliminate entirely) the occurrence of shock loading in the system. In this way, the fixturing of the WEC device to the buoy would bear minimal loading and would create little risk of damage to the structural integrity of the buoy.

Importantly, in the case of any catastrophic failure to the WEC device, the only consequence is the loss of its power contribution to the buoy. If a failure occurred such that the rotational system could still move, the device would continue to damp the pitching/rolling of the buoy – which is likely a net positive from the perspective of signals and sensors. If a complete failure of the system

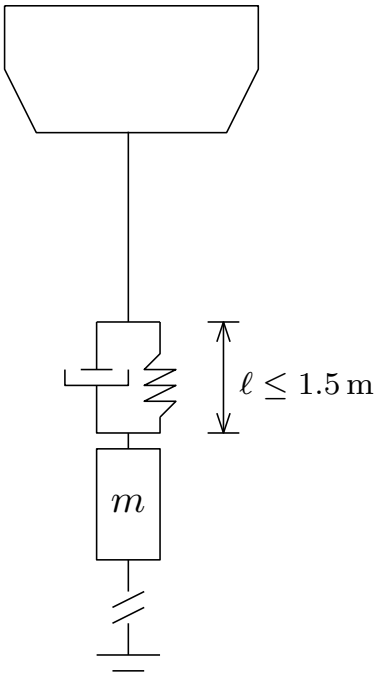

Figure 3-4 In-line power take-off wave energy converter concept.

occurred such that the rotational system locked, the WEC would become static mass, the equivalent of a ballast.

Estimates of power take off from a pitching resonator vary heavily with the hydrodynamics of the buoy. Further investigation of these response characteristics need to be investigated to provide a precise number, but early simulation indicate the expected average electrical power output to be on the order of 10-100 W.

3.3. Concept B1: in-line PTO

Figure 3-4 shows the basic concept for an in-line PTO, which converts work done by the surface buoy on the mooring riser into electricity. This concept is similar to a number of commercial WEC designs (see, e.g., AquaHaromnics[6], CorPower[7]), but is unique due to the presence of the stretch hose and NSIF. As illustrated in Figure 1-2b, the stretch hose acts as spring to decouple motion of the surface buoy from the MFN, thus decreasing loading in the system while allowing the surface buoy to follow the free surface.

The stretch hose in the CSM mooring riser has been developed by WHOI over many deployments and extensively tested to determine its performance [21, 22, 15]. Figure 3-5 shows the measured strain behavior of the stretch hose along with several local linear approximations. These linear approximations have slopes that range from 0.1 to 2.4 kN/m – which is one to two orders of magnitude lower than the heave hydrostatic stiffness of the surface buoy (86 kN/m). Thus, the stretch

[6]AquaHarmonics: https://aquaharmonics.com/
[7]CorPower: https://corpowerocean.com/

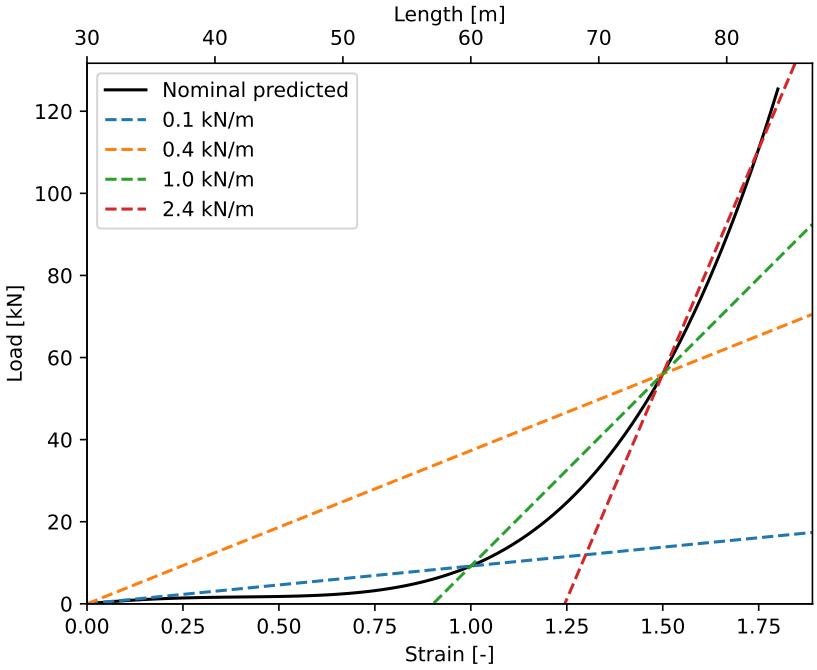

Figure 3-5 Stretch hose strain behavior with local linear approximations (data provided by WHOI).

hose is very well suited to allowing for free motion of the surface float while limiting loading in the mooring riser, but this behavior also limits the degree to which an in-line PTO within the mooring riser can generate electricity.

This result is also evident in the design analysis performed by WHOI ahead of the MAB deployment [2], as shown in Table 3-2. Here, Env-B is the most typical sea state; in this scenario, we can see that the section of the mooring riser between the NSIF and the surface buoy will see a standard deviation in tension of less the 1 kN. Lower sections of the mooring riser will see even lower tension fluctuations (0.1 to 0.2 kN). The higher loading fluctuations in the uppermost section of the mooring riser (the EM chain section; see Figure 1-2a) are likely due to the non-negligible mass and drag properties of the NSIF. For this reason, this uppermost section of the mooring riser is considered most suitable for an in-line PTO.

Based on the MBARI-WEC [13], which is of a similar scale and has been developed over 10+ years to operate robustly, and experience from the WHOI design and deployment/recovery teams, the following key aspects were identified for such an in-line PTO system:

- **Handle side loading** - Side loading will occur in addition to the power producing tension loading; any PTO system would need to cope with this side loading.
- **Short physical length** - Because of the deployment/recovery processes used for the surface buoy and NSIF (see Appendix B), the flexible EM chain between these bodies needs to be long enough to set the surface buoy and NSIF side-by-side on the ship's stern. The maximum length of the PTO to avoid substantial changes to the deployment/recovery procedure is 1-1.5 m (see Figure 3-4).

Table 3-2 Proteus-DS modeling results for Coastal Surface Mooring in 100 m water ("CP11NOSM") at Mid-Atlantic Bight, reproduced with permission from [2].

		Env-A	Env-B	Env-C	Env-D
Watch circle radius	m	28	64	165	177
NSIF Angle (mean)	deg	4	10	49	52
NSIF Angle (std)	deg	1	4	5	6
NSIF Angle (max)	deg	5	20	67	79
Buoy tension (mean)	N	2342	3225	10311	15934
	lb	527	725	2318	3582
Buoy tension (std)	N	166	995	2420	4263
	lb	37	224	544	958
Buoy tension (max)	N	2629	6939	18266	35970
	lb	591	1560	4106	8086
Hose tension (at upper HIB) (mean)	N	243	1160	9620	15600
	lb	55	261	2163	3507
Hose tension (at upper HIB) (std)	N	90	197	1150	2800
	lb	20	44	259	629
Hose tension (at upper HIB) (max)	N	403	1690	12800	27500
	lb	91	380	2878	6182
Anchor tension (mean)	N	237	1221	9913	16062
	lb	53	274	2229	3611
Anchor tension (std)	N	129	111	1359	3105
	lb	29	25	306	698
Anchor tension (max)	N	475	1400	13819	29432
	lb	107	315	3107	6617
Angle at anchor (from vertical)	deg	41	53	64	66

- **Handle end-stop events** - Due to the wide range of conditions and short permitted travel, end-stop events in which the PTO reaches is maximum linear travel should be expected.

- **Pass conductors** - To carry power and data, forty-six conductors currently travel between the surface buoy and the NSIF; twenty-two conductors travel between the NSIF and MFN. An in-line PTO would need to accommodate this conductors.

- **Handle a wide range of mean tensions** - As shown in Table 3-2, the mooring riser experiences mean tensions one order of magnitude greater than the variations which are the power producing component. The PTO would need to manage these large mean tensions while still generating power from the much lower magnitude tension fluctuations.

An uncoupled analysis can be performed to provide an upper bound to the amount of power that an in-line PTO located between the surface buoy and EM chain could provide. If, as shown in Table 3-2, the standard deviation of the tension is 995 N and this were assumed to be caused by a

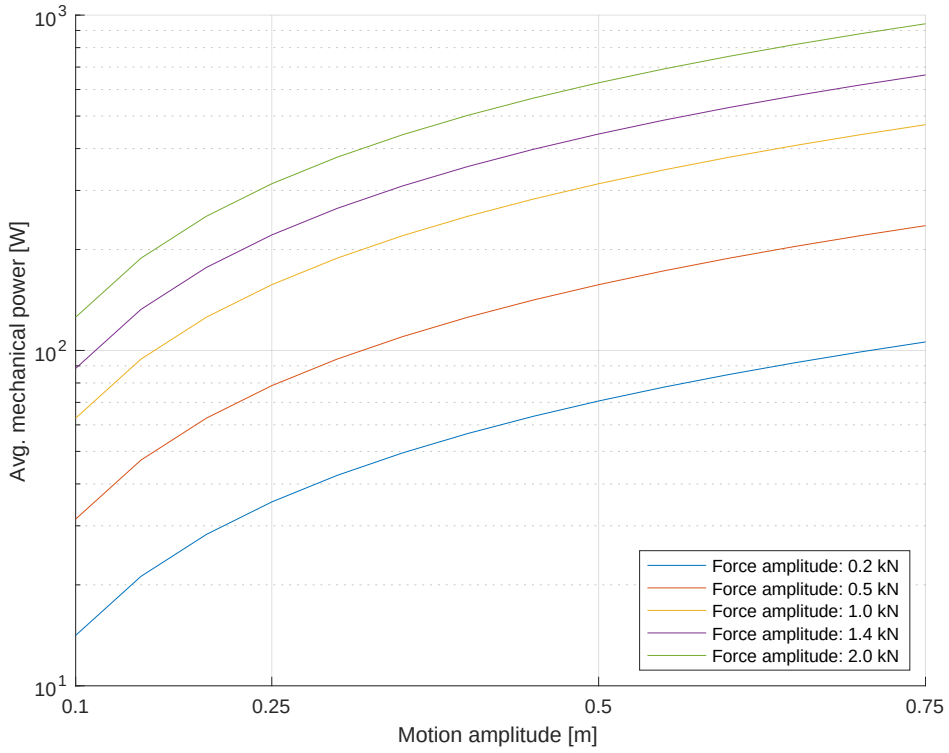

Figure 3-6 In-line PTO concept mechanical power generation based on motion and tension fluctuation amplitude.

sinusoidal variation about the mean, the amplitude of that sinusoid would be 1.4 kN ($\sigma = \frac{1}{\sqrt{2}} \|\hat{u}\|$). The average power absorbed from a damper on harmonic motion is

$$\bar{P}_b = \frac{1}{2} b \|\hat{u}\|^2, \tag{6}$$

where b is the damping and u is the velocity. Assuming a period 5 s for a regular wave and a range of force amplitudes (225 N and 1.4 kN correspond roughly to "Env-A" and "Env-B" in Table 3-2, respectively), we can calculate the average mechanical power produced as a function of motion amplitude (see Figure 3-6). The motion amplitude is of course important given the previously discussed limitation on stroke length.

Note that this is a static analysis (i.e., the motion imagined from a PTO does not affect the force). However, since the motion imagined is small it follows that the effect is likely small. A WEC-Sim model [17] was also developed to assess Concept B1 and showed similar results.

4. CONCLUSIONS AND FUTURE WORK

Table 4-1 shows a matrix assessing the viability of each concept against the criteria developed in Section 1.2. Each column of the table pertains to one of the three wave energy concepts considered and discussed in Section 3; each row captures a different design criterion (see Section 1.2).

Table 4-1 Wave energy converter system concept assessment matrix (see Section 3 for further details).

	A1: Linear sliding mass	A2: Pitch resonator	B1: In-line PTO
Power generation	*10-100 W*	*10-100 W*	*10-1,000 W*
Avoid catastrophic failures	*PTO failure might affect measurements (e.g., static list angle), unlikely to result in failure of entire mooring*	*PTO failure unlikely to negatively affect mooring or measurements, may even stabilize platform in pitch/roll*	*Failure of the PTO could potentially result in failure of the entire mooring*
Safe mode	*Easily implemented*	*Easily implemented*	*Medium difficulty to implement*
Not affect measurements	*Unlikely to affect measurements, may improve measurement quality by reducing buoy pitch/roll motion*	*Unlikely to affect measurements, may improve measurement quality by reducing buoy pitch/roll motion*	*May affect measurements due to increased motion of the NSIF and disturbance or blockage of flow of NSIF instruments*
Maintain current operational requirements	*Little to no effect on current operational procedures*	*Little to no effect on current operational procedures*	*Potential to have some effect on deployment procedures, but design can likely be targeted to minimize this*
Engineering challenges	*Linear stage may be challenging to locate within existing buoy layout; mean slider location will not be perfectly centered; linear motion platforms are generally more difficult to design than purely rotational platforms*	*Narrow-banded response may challenge robustness of performance; magnetic spring is a relatively immature technology*	*Deployment/recovery challenges; need to pass conductors; biofouling; side-loading*

Concept B1 is expected to have higher power generation potential than Concepts A1 and A2, but has higher risks in terms of engineering challenges, effects on measurements, integrity of mooring riser, and deployment/recovery. Concept A1 is more challenging to model and control, and therefore has more uncertainty/risk in terms of engineering and performance than Concept A2.

Based on these factors and the overall assessment captured in Table 4-1, our team currently views Concept A2 ("pitch resonator") as the most promising option, followed by Concept B1 ("in-line PTO"). The next steps of this project would be to down-select between Concepts A2 and B1, and then pursue a detailed design, assemble the prototype, perform shakedown and integration testing, and deploy a wave energy equipped CSM system for at-sea testing.

REFERENCES

[1] Seongho Ahn, Vincent S. Neary, Mohammad Nabi Allahdadi, and Ruoying He. Nearshore wave energy resource characterization along the east coast of the united states. *Renewable Energy*, 172:1212–1224, 2021.

[2] Derek Buffitt, Don Peters, and Al Plueddemann. Analysis of Pioneer MAB Coastal Surface Mooring. Technical Report 3102-00026, Woods Hole Oceanographic Institution, 02 2023.

[3] Dawei Che, Bertrand Dechant, Alex Hagmüller, and Jonathan Z Bird. A multi-stack variable stiffness magnetic torsion spring for a wave energy converter. In *2022 IEEE Energy Conversion Congress and Exposition (ECCE)*, pages 1–6. IEEE, 2022.

[4] H. Ming Chen and Donald R. DelBalzo. Linear sliding wave energy converter. In *OCEANS 2015 - Genova*, pages 1–6, 2015.

[5] J. Cordonnier, F. Gorintin, A. De Cagny, A.H. Clément, and A. Babarit. Searev: Case study of the development of a wave energy converter. *Renewable Energy*, 80:40–52, 2015.

[6] J.P. Den Hartog. *Mechanical Vibrations*. Civil, Mechanical and Other Engineering Series. Dover Publications, 1985.

[7] Chris Dizon and Ted Brekken. Relationship Between Power Output and Chaotic Behavior of a Pendulum PTO WEC. *IFAC-PapersOnLine*, 55(27):132–137, 2022. 9th IFAC Symposium on Mechatronic Systems MECHATRONICS 2022.

[8] Chris Dizon, Robert J. Cavagnaro, Bryson Robertson, and Ted K. Brekken. Modular horizontal pendulum wave energy converter: Exploring feasibility to power ocean observation applications in the U.S. Pacific Northwest. *IET Renewable Power Generation*, 15(14):3354–3367, 2021.

[9] D.V. Evans. Maximum wave-power absorption under motion constraints. *Applied Ocean Research*, 3(4):200–203, 1981.

[10] Daniele Giovanni Gioia, Edoardo Pasta, Paolo Brandimarte, and Giuliana Mattiazzo. Data-driven control of a pendulum wave energy converter: A Gaussian process regression approach. *Ocean Engineering*, 253:111191, 2022.

[11] Mark A. Grosenbaugh, Walter Paul, Dan Frye, and Norman Farr. Development of synthetic fiber-reinforced electro-optical-mechanical cables for use with moored buoy observatories. *IEEE Journal of Oceanic Engineering*, 31(3):574–584, 2006.

[12] Jørgen Hals, Johannes Falnes, and Torgeir Moan. Constrained Optimal Control of a Heaving Buoy Wave-Energy Converter. *Journal of Offshore Mechanics and Arctic Engineering*, 133(1):011401, 11 2010.

[13] Andrew Hamilton, François Cazenave, Dominic Forbush, Ryan G. Coe, and Giorgio Bacelli. The MBARI-WEC: a power source for ocean sensing. *Journal of Ocean Engineering and Marine Energy*, 7(2):189–200, 2021.

[14] Mahmodul Hasan Maheen and Yingchen Yang. Wave energy converters with rigid hull encapsulation: A review. *Sustainable Energy Technologies and Assessments*, 57:103273, 2023.

[15] James D. Irish, Walter Paul, and David M. Wyman. The determination of the elastic modulus of rubber mooring tethers and their use in coastal moorings. Technical Report WHOl-2005-10, Woods Hole Oceanographic Institution, Woods Hole, Massachusetts, Dec 2005.

[16] Calum Kenny and Jim McNally. Internal reaction mass taxonomy and narrow-down study. 9 2022.

[17] Michael Lawson, Yi-Hsiang Yu, Kelley Ruehl, Carlos Michelen, et al. Development and demonstration of the WEC-Sim wave energy converter simulation tool. In *Proceedings of the 2nd Marine Energy Technology Symposium (METS 2014)*, Seattle, WA, April 2014.

[18] Pozzi Nicola, Bracco Giovanni, Passione Biagio, Sirigu Sergej Antonello, Vissio Giacomo, Mattiazzo Giuliana, and Sannino Gianmaria. Wave tank testing of a pendulum wave energy converter 1:12 scale model. *International Journal of Applied Mechanics*, 09(02):1750024, 2017.

[19] K. Ogata. *System Dynamics: Pearson New International Edition*. Pearson Education, 2013.

[20] Edoardo Pasta, Fabio Carapellese, and Giuliana Mattiazzo. Deep neural network trained to mimic nonlinear economic model predictive control: an application to a pendulum wave energy converter. In *2021 IEEE Conference on Control Technology and Applications (CCTA)*, pages 295–300, 2021.

[21] Walter Paul. Design considerations for stretch conductors in oceanographic moorings. Technical Report WHOI-95-15, Woods Hole Oceanographic Institution, Woods Hole, Massachusetts, Dec 1995.

[22] Walter Paul. Hose elements for buoy moorings: Design, fabrication and mechanical properties. Technical Report WHOI-2004-06, Woods Hole Oceanographic Institution, Woods Hole, Massachusetts, July 2004.

[23] A. Plueddemann, A. Macdonald, and A. Ramsey. CGSN Site Characterization: Pioneer Mid-Atlantic Bight Array. Technical Report 3210-00007, Woods Hole Oceanographic Institution, 02 2023.

[24] Troy Shinbrot, Celso Grebogi, Jack Wisdom, and James A. Yorke. Chaos in a double pendulum. *American Journal of Physics*, 60(6):491–499, 06 1992.

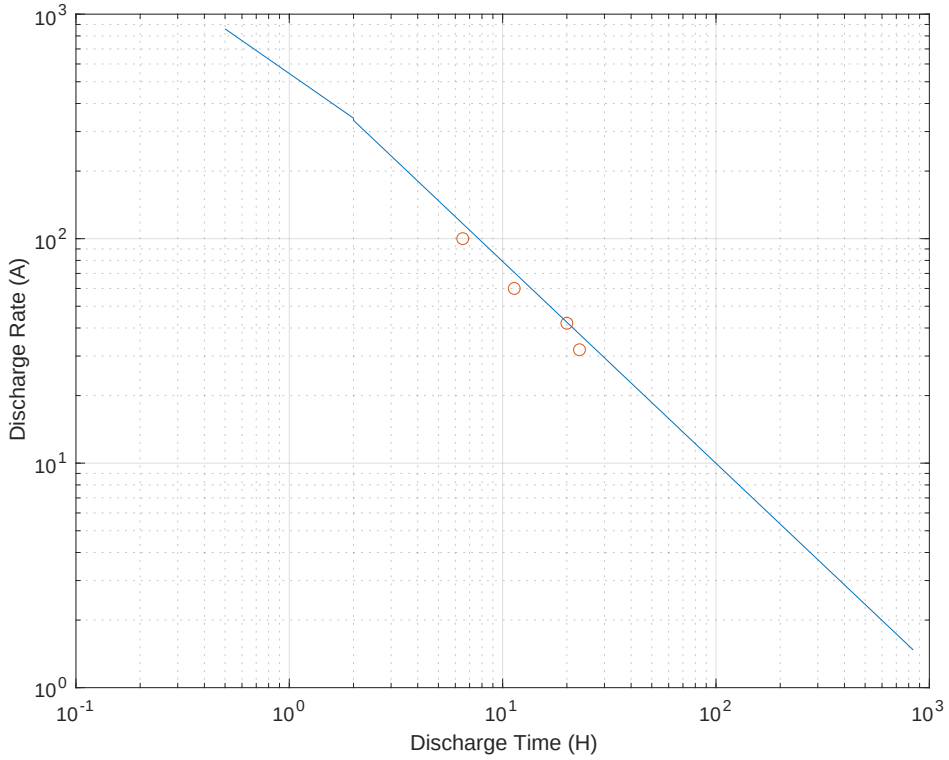

Figure A-1 Peukert curve for 4-P GPL-4DL absorbent glass mat battery.

A. BATTERY STATE OF CHARGE ESTIMATION

The temperature has a number of influences on the battery state of charge (SoC) and state of health (SoH).

- Charging voltages are increased at lower temperatures
- Amp-hour (AH) capacity is decreased at lower temperatures
- Battery life (number of charge-discharge cycles) is increased with lower temperatures

Open-circuit voltage (OCV) is minimally impacted by temperature (32 mV influence for a 24 V battery over a 50-80°F range), whereas charging voltages increase by 900 mV over the same range. OCV is the voltage of the battery at rest without having been loaded or charged for at least 4 hours – it is therefore not practical to directly measure this in-situ. The discharge rates observed in the data are very low (2 A max). This corresponds to a 600 H rate for the 4P setup (Figure A-1). Between 100-30% SoC, the discharge voltage curves closely follow the SoC/OCV relationship (Figure A-2) when the discharge time is longer than 8H. This trend is likely accurate to $\pm 10\%$ SoC at best. Below 30% SoC, discharge voltage drops rapidly.

The internal series resistance (ISR) for the battery should only be $\sim 2\text{m}\Omega$; according to the datasheet. Based on the data, we estimate series resistance to be between 300-600mΩ. This could be due to an external resistance in the setup.

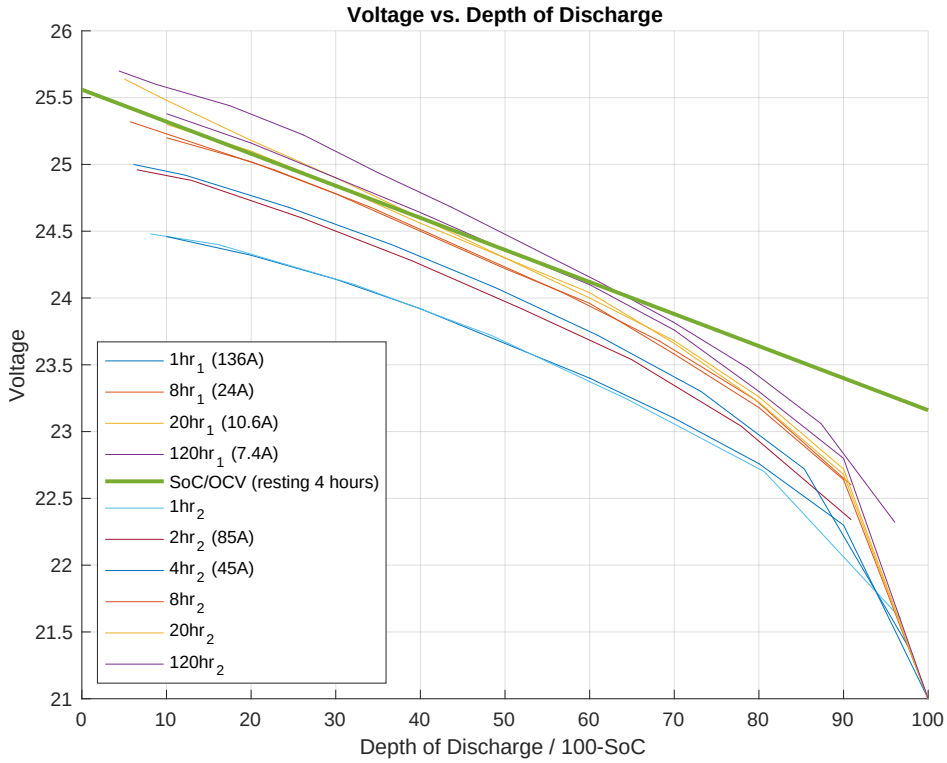

Figure A-2 Battery voltage versus depth of charge.

An ANOVA analysis was performed on the measured voltage prediction from a quadratic current+temperature relationship plus terms for integrals of current and temperature for historical influences (see Table A-1). The quadratic term was used to test first order effects of temperature on the series resistance. The result was that current was by far the largest contributor to explain the variances observed in the voltage. Subsequently, the analysis was reframed with only a current relationship to find the R_s that best explains the correlation between voltage and current ($R_s = 368\text{m}\Omega$). Including this should reduce the error in estimating OCV based on the available data.

Table A-1 Battery state of charge analysis of variance.

	SumSq	DF	MeanSq	F	pValue
Current	146.3017	1	146.3017	1854.5952	6.8313e-222
Temperature	0.00080655	1	0.00080655	0.010224	0.91948
intT	0.92015	1	0.92015	11.6643	0.00066524
Charge	10.152	1	10.152	128.6917	5.4079e-28
Current:Temperature	0.55035	1	0.55035	6.9765	0.0084004
Current^2	3.1703	1	3.1703	40.1886	3.6234e-10
Temperature^2	9.0472	1	9.0472	114.6871	2.7381e-25
Error	71.8652	911	0.078886	1	0.5

B. DEPLOYMENT SEQUENCE

Figure B-1 and Figure B-2 show key steps and stages in the CSM deployment sequence, particularly with respect to the NSIF and surface buoy.

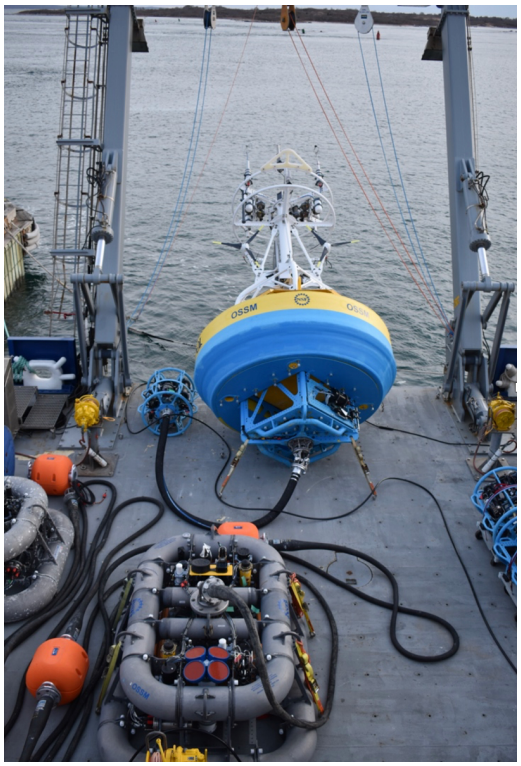

(a) The mooring components are assembled and laid out on deck.

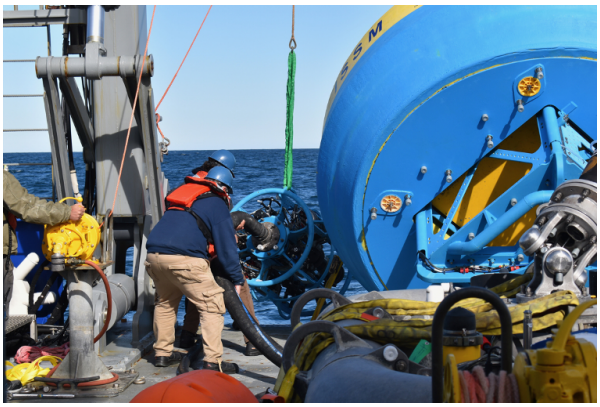

(b) The NSIF is maneuvered aft of the buoy.

Figure B-1 Coastal Surface Mooring deployment sequence.

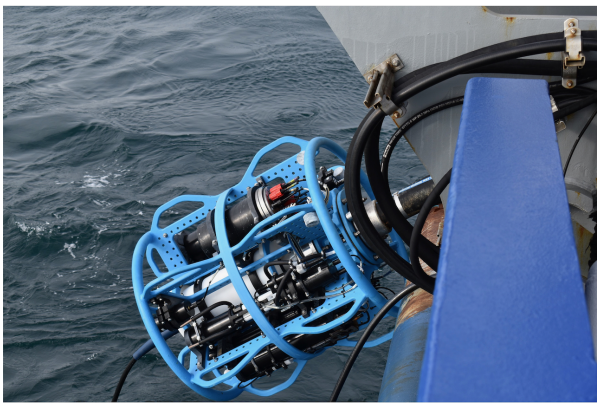

(a) The NSIF is hung over the transom with a stopper line.

(b) The buoy is lifted clear of the deck, shifted aft as the A-frame is moved outboard, and then lowered to the water line and released. At the same time the NSIF is lowered into the water with a slip line.

(c) The buoy trails behind as ship steams ahead, EM cable and stretch hoses are fed aft, and buoyancy elements are transferred over the transom with the A-frame and released.

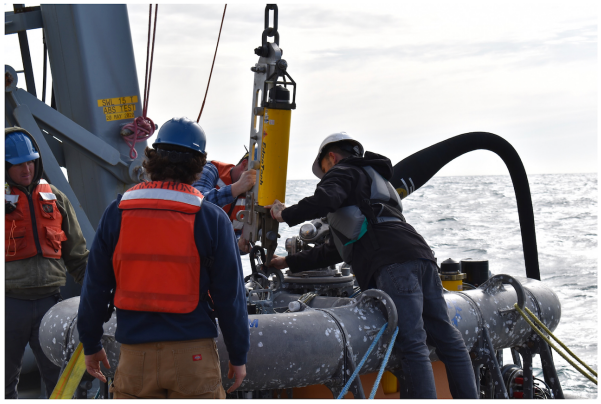

(d) With all mooring components except the MFN trailing behind the ship, a lowering release is connected to the ship's trawl winch in order to allow controlled lowering of the MFN. The MFN is lifted clear of the deck, shifted outboard with the A-frame, and lowered into the water. The MFN is released when it is about 30 m above the sea floor.

Figure B-2 Coastal Surface Mooring deployment sequence (cont.).

C. OTHER WAVE ENERGY CONCEPTS

Figure C-1 shows other concepts considered for the wave energy system during our design process and describes why each of these concepts was not pursued further.

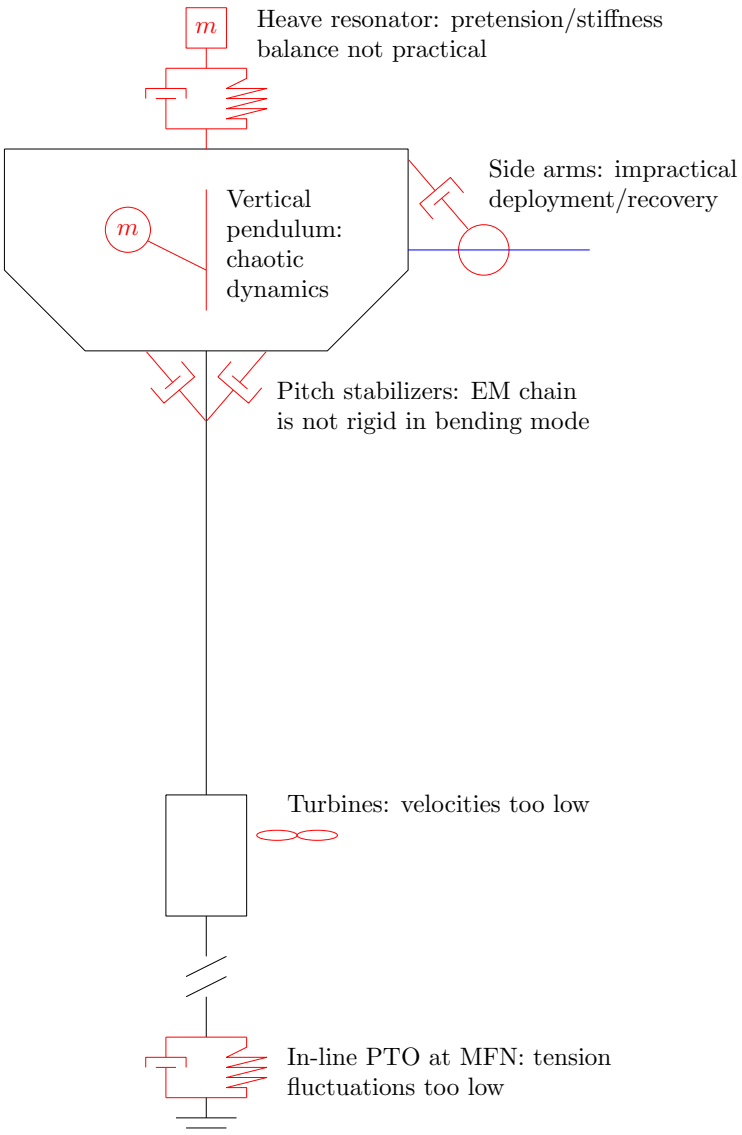

Figure C-1 Other wave energy converter concepts considered.

DISTRIBUTION

Email—Internal

Name	Org.	Sandia Email Address
Technical Library	1911	sanddocs@sandia.gov

Sandia National Laboratories

Sandia National Laboratories is a multimission laboratory managed and operated by National Technology & Engineering Solutions of Sandia LLC, a wholly owned subsidiary of Honeywell International Inc., for the U.S. Department of Energy's National Nuclear Security Administration under contract DE-NA0003525.